An Evaluation of HIRS Near-Surface Air Temperature Product in the Arctic with SHEBA Data

GE PENG

Cooperative Institute for Climate and Satellites–North Carolina, North Carolina State University, and NOAA/National Centers for Environmental Information, Asheville, North Carolina

LEI SHI

NOAA/National Centers for Environmental Information, Asheville, North Carolina

STEVE T. STEGALL AND JESSICA L. MATTHEWS

Cooperative Institute for Climate and Satellites–North Carolina, North Carolina State University, and NOAA/National Centers for Environmental Information, Asheville, North Carolina

CHRISTOPHER W. FAIRALL

NOAA/Earth System Research Laboratory, Boulder, Colorado

(Manuscript received 29 October 2015, in final form 15 January 2016)

ABSTRACT

The accuracy of cloud-screened 2-m air temperatures derived from the intersatellite-calibrated brightness temperatures based on the High Resolution Infrared Radiation Sounder (HIRS) measurements on board the National Oceanic and Atmospheric Administration (NOAA) Polar-Orbiting Operational Environmental Satellite (POES) series is evaluated by comparing HIRS air temperatures to 1-yr quality-controlled measurements collected during the Surface Heat Budget of the Arctic Ocean (SHEBA) project (October 1997–September 1998). The mean error between collocated HIRS and SHEBA 2-m air temperature is found to be on the order of 1°C, with a slight sensitivity to spatial and temporal radii for collocation. The HIRS temperatures capture well the temporal variability of SHEBA temperatures, with cross-correlation coefficients higher than 0.93, all significant at the 99.9% confidence level. More than 87% of SHEBA temperature variance can be explained by linear regression of collocated HIRS temperatures. The analysis found a strong dependency of mean temperature errors on cloud conditions observed during SHEBA, indicating that availability of an accurate cloud mask in the region is essential to further improve the quality of HIRS near-surface air temperature products. This evaluation establishes a baseline of accuracy of HIRS temperature retrievals, providing users with information on uncertainty sources and estimates. It is a first step toward development of a new long-term 2-m air temperature product in the Arctic that utilizes intersatellite-calibrated remote sensing data from the HIRS instrument.

1. Introduction

Surface temperature in the Arctic warmed at a rate nearly twice the global average since 1950 (Hassol 2004; Karl et al. 2015). The temperature increase has been especially large during winter. In Alaska, winter air temperatures observed by land-based weather stations have shown an increase of 3°–4°C over the last 50 years (Hassol 2004). An additional 4°–7°C of Arctic warming is projected over the next 100 years, posing extreme challenges to sustainability and resilience of the Arctic system while potentially bringing opportunities, such as access to new sources of natural resources and ocean routes (Hassol 2004; Jeffries et al. 2014). Since the 1970s satellite measurements have recorded a 10%–15% decade^{-1} decrease in the Arctic annual minimum sea ice extent (Comiso and Nishio 2008; Cavalieri and Parkinson 2012; Peng et al. 2013),

Corresponding author address: Ge Peng, CICS-NC/NCEI, 151 Patton Avenue, Asheville, NC 28801-5001.
E-mail: ge.peng@noaa.gov

DOI: 10.1175/JTECH-D-15-0217.1

faster than most climate model predictions (Stroeve et al. 2012). Sea ice is also thinning as the result of multiyear sea ice loss (e.g., Comiso 2012), with the temperature-forced ice volume decline accounting for three-quarters of the -4% decade^{-1} total modeled trend (Rothrock and Zhang 2005).

Polar oceans are an important part of the world's oceans in understanding and monitoring weather and climate variability. For example, a warmer Arctic could potentially weaken or halt the Gulf Stream, which could result in colder weather to northwestern Europe (Hassol 2004; highlights can be found online at http://www.greenfacts.org/en/arctic-climate-change/). Understanding and quantifying the role of polar ocean variability in global weather and climate changes require accurate global surface flux products (U.S. CLIVAR Scientific Steering Committee 2013; Bourassa et al. 2013; NRC 2006).

Significant discrepancies exist in surface analyses from major numerical weather prediction (NWP) centers and model predictions of future climate conditions (e.g., Bauer et al. 2016; Randall et al. 1998). Bauer et al. (2016) pointed out that the discrepancies may be due to the fact that station networks are often limited to coastlines and inhabited areas in polar areas. Model analyses (as initial conditions for model forecasts or as first guesses for reanalyses) may also inherit a strong dependence on station representativeness, and model verifications may lack independence, since measurements from the same networks are used in both assimilation and verification (Bauer et al. 2016). Trends of 2-m air temperature exhibit distinct spatial variability over the Arctic (Rigor et al. 2000). The sparsity of those surface-based stations may lead to underrepresentativeness of spatial variability in model reanalyses (S. Stegall 2015, personal communication). Utilizing satellite measurements may help alleviate some of these issues and help improve our understanding of weather and climate systems in the Arctic and their interactions with extratropical and/or tropical systems.

The remote and extreme Arctic environment has made it extremely difficult to measure air–sea and ice fluxes. This in turn hinders our estimates of surface temperature trends and understanding of related physical processes and feedbacks (Cowtan and Way 2014; Karl et al. 2015; Bourassa et al. 2013). It also limits our ability to monitor changes that are already underway in the region. The availability of satellite data products makes it possible to observe and monitor changes of sea ice extent (e.g., Stroeve et al. 2012; Comiso 2012), something that is not possible from in situ measurements alone. However, accurate surface flux products in the Arctic are still lacking, especially for long-term and intersatellite-calibrated time series.

Surface and near-surface air temperatures are commonly used to refer to air temperature either at the surface or at the reference height of 2 or 10 m. They are surface flux variables and important for understanding and monitoring changes in the radiation balance and hydrological cycle in the polar region. As one of the 10 high-priority measurements identified in NRC (2001), long-term and consistent records of temperature are also essential for monitoring and examining the response to those changes and their impact on future climate change (NRC 2001).

In this paper, we compare two sets of near-surface air temperature measurements: 1) swath cloud-screened air temperatures at 2-m height (T2m) derived from the intersatellite-calibrated brightness temperatures based on the High Resolution Infrared Radiation Sounder (HIRS) measurements on board the National Oceanic and Atmospheric Administration (NOAA) Polar-Orbiting Operational Environmental Satellite (POES) series, and 2) 1-yr quality-controlled T2m during the Surface Heat Budget of the Arctic Ocean (SHEBA) project (October 1997–September 1998). The comparison is carried out to evaluate the accuracy of the HIRS retrievals and their dependency on different cloud conditions and to establish a baseline for a long-term near-surface remote-sensed air temperature product for the Arctic. The statistical characteristics of the comparison provide users with information on product uncertainty sources and estimates.

2. Data outline

a. HIRS swath near-surface temperatures

The HIRS instrument has been making routine measurement of the atmosphere since 1978 from more than a dozen satellites. Measurements from individual satellites are intercalibrated to form a temporary homogeneous time series (Shi et al. 2008; Shi 2011; Shi et al. 2012). HIRS has 20 spectral channels, including 19 infrared channels and one visible channel. The near-surface air temperatures are derived using a neural network approach as a part of a global atmospheric profile dataset (for more details see Shi et al. 2015, manuscript submitted to *Remote Sens.*). The input consists of brightness temperature measurements from the HIRS channels with weighting function peaking at or near the surface as well as the surface emissivity. Among these HIRS channels, channels 7, 8, and 10 are designed to measure the surface and lower-atmospheric temperature and humidity (Shi et al. 2008). Channel 8, as a window channel with the wavelength of 11.11 μm, senses temperature at the surface. The weighting function of channel 7 (13.35 μm) peaks near the surface for

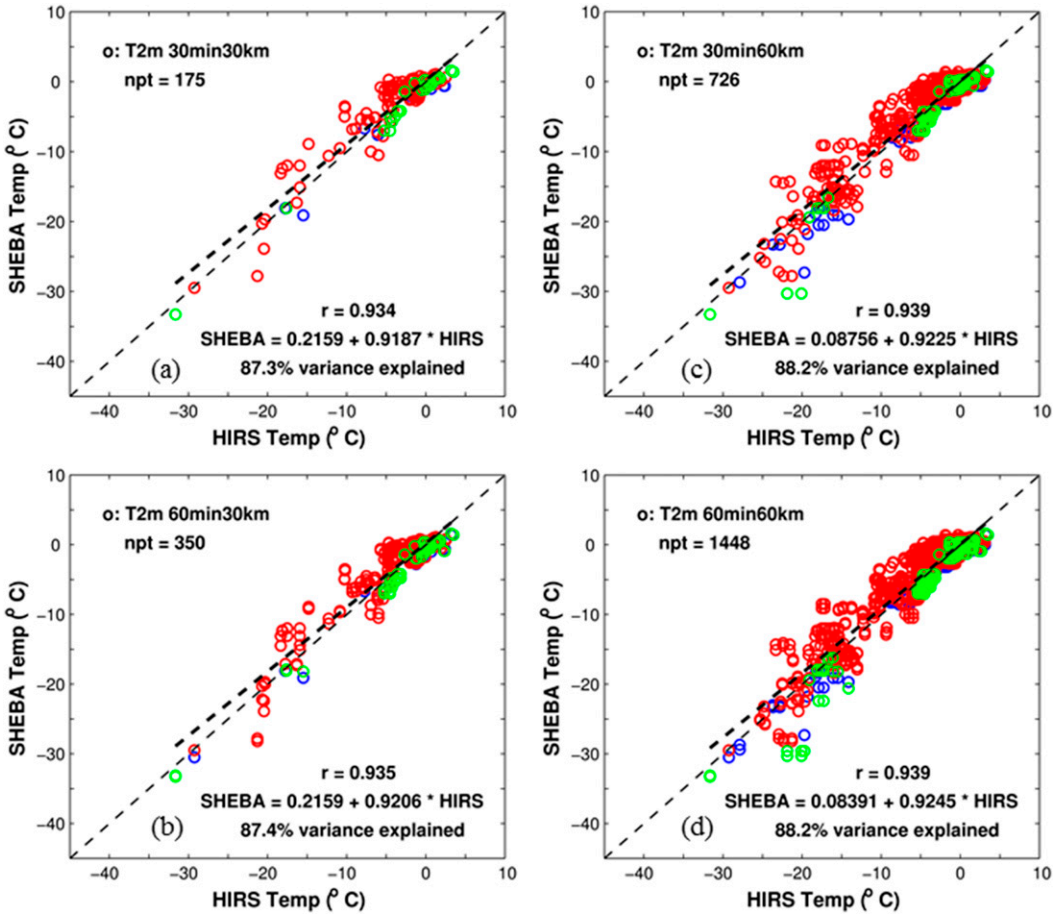

FIG. 1. Scatter diagram of collocated HIRS and SHEBA T2m: (a) a temporal radius of 30 min and a spatial radius for collocation of 30 km, i.e., 30min30km case; (b) the 60min30km case; (c) the 30min60km case; and (d) the 60min60km case. The color code is for overcast (red: SHEBA cloud fractions $\geq 80\%$), clear-sky (green: SHEBA cloud fractions $\leq 10\%$), and cloudy (blue: $10\% <$ SHEBA cloud fractions $< 80\%$). The cross-correlation coefficient between the two time series is denoted in the plot by "*r*." The linear regression is in the plot along with the percentage of SHEBA temperature variance explained by the linear regression of HIRS temperatures. The threshold of 80% for the overcast condition is subjective and is not consistent with the meteorological overcast definition. It is based on examining the characteristics of HIRS–SHEBA T2m dependence on SHEBA cloud fractions (see Fig. 2). This grouping is to aid statistical analysis and discussion.

measuring temperature, and that of channel 10 (12.56 μm) peaks near the surface for measuring humidity. The combination of these channels provides information for retrieving T2m. The current study focuses on T2m retrievals produced by Shi et al. (2015, manuscript submitted to *Remote Sens.*), for the period of one year—that is, from 1 October 1997 through 30 September 1998—from the *NOAA-14* measurements.

b. *Integrated SHEBA dataset*

The SHEBA project was a multiagency and interdisciplinary effort with a yearlong field experiment in the Beaufort and Chukchi Seas (October 1997–October 1998). It produced a rich collection of atmospheric, oceanographic, and cryospheric measurements taken on a Canadian icebreaker frozen in the Arctic ice pack (Uttal et al. 2002; Persson et al. 2002). SHEBA data used in this comparison are from the SHEBA composite data observations product (downloaded from http://www.eol.ucar.edu/projects/sheba/). This dataset contains the hourly values of 31 parameters (Persson et al. 2002), including near-surface temperatures and cloud fractions used in this study.

3. Evaluation of HIRS T2m with SHEBA

a. *Sensitivity of collocating HIRS and SHEBA measurements*

The SHEBA data are point measurements, while HIRS are from space looking down at the nadir with a

TABLE 1. Statistics of collocated HIRS–SHEBA T2m difference.[a]

Collocation case	30min30km	60min30km	30min60km	60min60km
No. of records	175	350	726	1448
Mean (°C)	−0.610	−0.589	−0.465	−0.459
Margin of error[b] (°C)	0.316	0.226	0.157	0.112
Min(°C)	−6.747	−6.747	−9.019	−9.019
Max (°C)	6.509	6.909	10.225	10.225
STD (°C)	2.131	2.160	2.156	2.179
RMSE (°C)	2.217	2.239	2.206	2.226
Cross correlation	0.9345	0.9351	0.9389	0.9390
Significant confidence level (%)	99.9	99.9	99.9	99.9
Intercept (°C)/slope of linear regression	0.2159/0.9187	0.2159/0.9206	0.0876/0.9225	0.0839/0.9245
Variance explained (%)	87.32	87.44	88.15	88.18

[a] The mean, STD, and RMSE are computed using normalized 3D distance weights defined as $W_{xyt} = \{1 - [(\Delta x/Rx)^2 + (\Delta y/Ry)^2 + (\Delta t/Rt)^2]/3\}$, where Δx, Δy and Rx, Ry are the distances (km) between HIRS and SHEBA data points and the collocation radius in longitude and latitude directions, respectively. Terms Δt and Rt are the temporal distance (min) between HIRS and SHEBA data points and the collocation radius, respectively.

[b] The margin of error for the means is computed assuming a 95% level of confidence.

swath of 2160 km and a nominal resolution of 20 km. The collocation is carried out picking all HIRS measurements within specified spatial and temporal radii of each SHEBA data point. The choice of radius can be quite arbitrary except for consideration of SHEBA and HIRS temporal and spatial resolutions. The balance to strike is between the number of available collocated records for analysis and HIRS measurements being too far away from the targeted SHEBA location. To determine the robustness of basic statistics over collocation radius, the sensitivity to a spatial radius of 30 km versus 60 km and a temporal radius of 30 min versus 60 min was examined.

While some degree of sensitivity is observed, more so to spatial radius, they are not significant enough to alter the basic overall characteristics (Fig. 1; Table 1). As shown in Fig. 1, the number of the available HIRS–SHEBA collocated data points is greatly reduced when going from the 60min60km case to the 30min30km case, that is, from 1448 to 175. The minimum/maximum of HIRS–SHEBA T2m difference for the 30min60km and 60min60km cases are higher, which slightly affects the mean bias, but with smaller margin of error due to increased collocated data points (Table 1). The standard deviation (STD) and root-mean-square error (RMSE) values of the HIRS and SHEBA T2m differences, which measure the degree of variation from the mean of the HIRS–SHEBA differences and the spread of HIRS measurement to SHEBA, respectively, are fairly similar for all four cases. So are the cross-correlation coefficients r of collocated HIRS and SHEBA time series (Table 1); all are significant at the 99.9% confidence level.

b. Sensitivity to cloud contamination

As an infrared sensor, HIRS cannot "see" through clouds. When clouds are present, HIRS senses the temperature at cloud top. Therefore, to obtain temperature retrievals near the surface, it is necessary to remove cloudy HIRS pixels. This study uses HIRS retrievals that have been cloud screened by a neighboring variance method to remove pixels containing clouds (Jackson and Bates 2000) and further filtered with cloud products derived from the Advanced Very High Resolution Radiometer (AVHRR) measurements on board the same satellites (Heidinger et al. 2014).

When there are undistinguished clouds in a HIRS pixel, the cloud-top temperature becomes the retrieved temperature for the pixel. This temperature is usually lower than the near-surface temperature. However, in high latitudes, inversion layers are often present, and in such conditions the retrieved temperature can be overestimated due to cloud contamination. Unfortunately, cloud coverage is fairly persistent, particularly during summer seasons during SHEBA (Intrieri et al. 2002). This makes the neighboring variance method especially prone to errors in the Arctic.

To assess the impact of cloud cover on HIRS near-surface temperature retrievals, HIRS temperatures were compared with SHEBA measurements under clear, cloudy, and overcast conditions based on SHEBA cloud fractions. As shown in Fig. 2, the characteristics of HIRS–SHEBA differences are clearly affected by the amount of cloud cover present at the time of observations. For the two cases of 30-km spatial radius, clear-sky data points are compactly clustered around

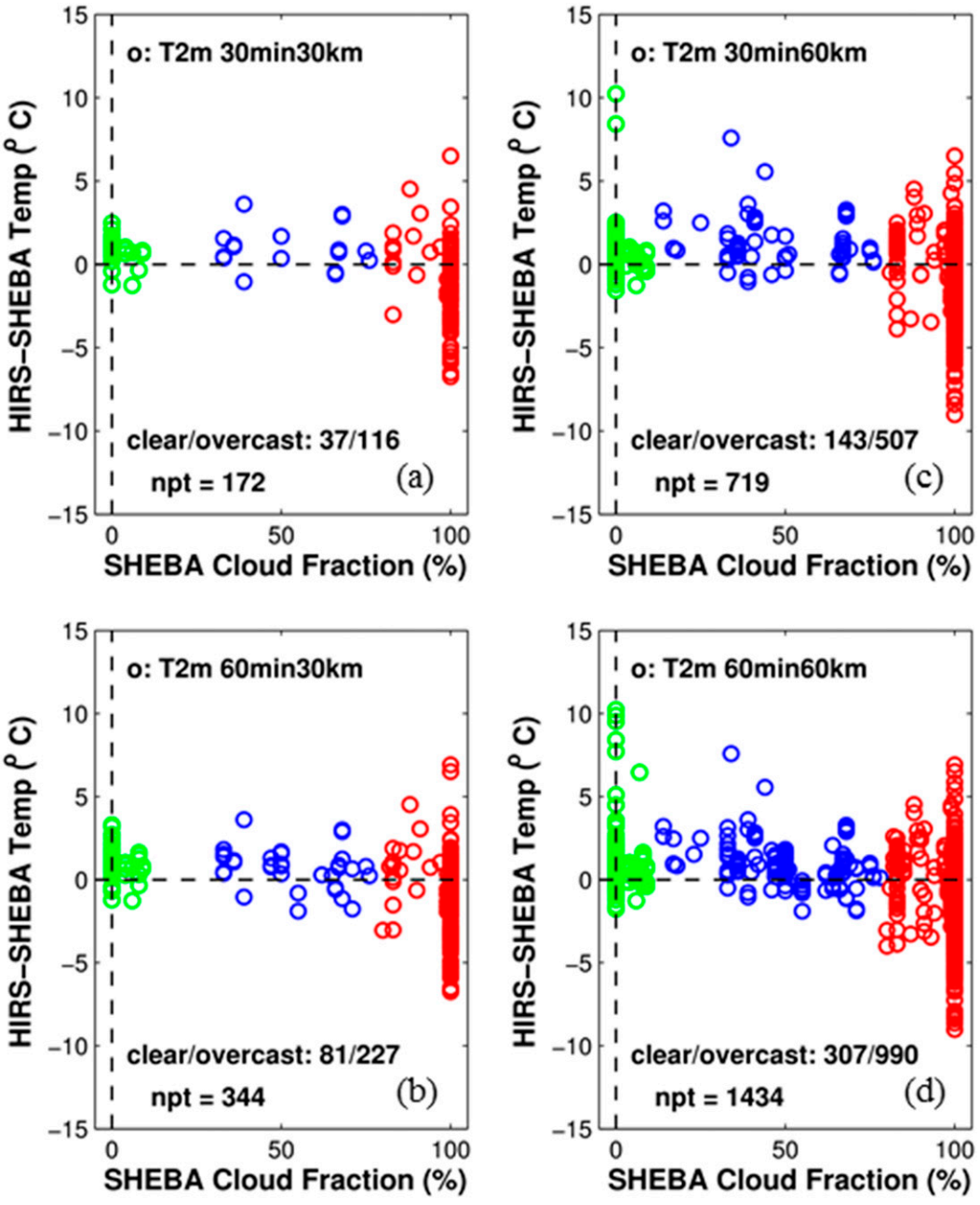

FIG. 2. Diagram of the dependency of HIRS and SHEBA T2m differences as a function of SHEBA cloud fractions: (a) the 30min30km case, (b) the 60min30km case, (c) the 30min60km case, and (d) the 60min60km case. The color code is for overcast (red: SHEBA cloud fractions $\geq 80\%$), clear-sky (green: SHEBA cloud fractions $\leq 10\%$), and cloudy (blue: $10\% <$ SHEBA cloud fractions $< 80\%$).

zero, and the magnitude of the temperature differences are less than ±3.3°C with a positive bias of ~0.8°C (Figs. 2a,b; Table 2). A similar behavior can be observed for partly cloudy points with a slightly larger spread, ranging from −1.898° to 3.61°C (Fig. 2a,b; Table 2). The HIRS–SHEBA temperature differences for the overcast cells, on the other hand, tend to be even more spread out, ranging from −6.747° to 6.909°C with a negative bias of about −1.2°C (Figs. 2a,b; Table 2). Increased spatial radius tends to increase the spread of T2m differences with more outliers, more so for the clear-sky points (Figs. 2c,d; see RMSE values in Table 2), which is likely due to the mismatch of cloud conditions for the area outside of the HIRS

TABLE 2. Statistics of HIRS–SHEBA T2m difference in relation to SHEBA cloud conditions.

Case type	Cloud filter type	No. records[a]	Mean (°C)	Min (°C)	Max (°C)	STD (°C)	RMSE (°C)
30min30km	Clear	37	0.757	−1.264	2.476	0.777	1.084
	Cloudy	19	0.908	−1.042	3.610	1.121	1.443
	Clear/cloudy	56	0.808	−1.264	3.610	0.910	1.217
	Overcast	116	−1.203	−6.747	6.509	2.228	2.532
60min30km	Clear	81	0.888	−1.264	3.301	0.836	1.219
	Cloudy	36	0.666	−1.898	3.610	1.184	1.358
	Clear/cloudy	117	0.819	−1.898	3.610	0.962	1.263
	Overcast	227	−1.221	−6.747	6.909	2.257	2.566
30min60km	Clear	143	0.838	−1.568	10.225	1.139	1.414
	Cloudy	69	1.236	−1.042	7.586	1.465	1.916
	Clear/cloudy	212	0.972	−1.568	10.225	1.273	1.602
	Overcast	507	−1.049	−9.019	6.509	2.172	2.412
60min60km	Clear	307	1.0	−1.768	10.225	1.287	1.630
	Cloudy	137	0.932	−1.898	7.586	1.340	1.633
	Clear/cloudy	444	0.979	−1.898	10.225	1.304	1.631
	Overcast	990	−1.075	−9.019	6.909	2.188	2.438

[a] The total number of records under the clear, cloudy, and overcast conditions may be less than that of all collocated records. For example, the total number of records under these cloud conditions for the 60min60km case is 1434 and the total HIRS–SHEBA collocated record number is 1448. The difference is due to missing SHEBA cloud fraction measurements.

footprint, implying that spatial separation variability dominates.

Different characteristics for HIRS–SHEBA T2m differences are seen with and without overcast points (Figs. 1, 3; Table 2). Overall, the HIRS T2m retrievals tend to overestimate in the clear and cloudy conditions, when SHEBA cloud fractions are less than 80%. They tend to underestimate when SHEBA cloud fractions are greater than 80% (Table 2). There is no obvious trend in RMSE values for the overcast conditions in all four cases, denoting that cloud variability is dominating separation variability. Nevertheless, when overcast cells are removed, the results demonstrate more consistent statistical characteristics among these four cases. For example, higher cross-correlation coefficients and higher percentage variances are explained by the linear regressions (cf. Fig. 1 with Fig. 3), and the smaller RMSE values (comparing ''clear/cloudy'' with ''overcast'' rows in Table 2).

Other factors affecting this comparison include the method for measuring cloud fractions. The SHEBA cloud fractions are mostly manual visual measurements, that is, point measurements looking up by humans whose visual range is limited to about 5 km. Manual observations generally contain some degree of subjectivity. The impact of human subjectivity to this analysis, however, is minimal because cloud fractions are put into three categories—clear, cloudy, and overcast—and the distinctions among these categories are normally obvious. HIRS measurements, on the other hand, are from space looking down with a resolution of 20 km at the nadir and with an increased footprint toward the sides of scan lines. While satellite-based cloud fractions may be highly correlated with surface observations at time scales greater than 5 days, they are less so, and with higher uncertainty, at shorter scales (Schweiger et al. 2002). Thus, some inconsistency between cloud coverage categorization from those two measurements is expected. This situation is more likely to occur for the two larger spatial radius cases.

4. Summary and discussion

Cloud-screened HIRS 2-m air temperatures are compared with observations from the integrated and quality-controlled SHEBA dataset. This comparison is carried out to evaluate the accuracy of HIRS retrievals and to establish a baseline for a long-term near-surface remotely sensed air temperature product in the Arctic.

The mean error between collocated HIRS and SHEBA T2m is found to be on the order of 1°C, with a slight sensitivity to spatial and temporal radius for collocation. The HIRS temperatures capture the temporal variability of SHEBA temperatures well, with cross-correlation coefficients higher than 0.93, all significant at the 99.9% confidence level. For the 60min60km case, the linear regression of HIRS onto SHEBA T2m shows a near-zero intercept and a slope of 0.92, with more than

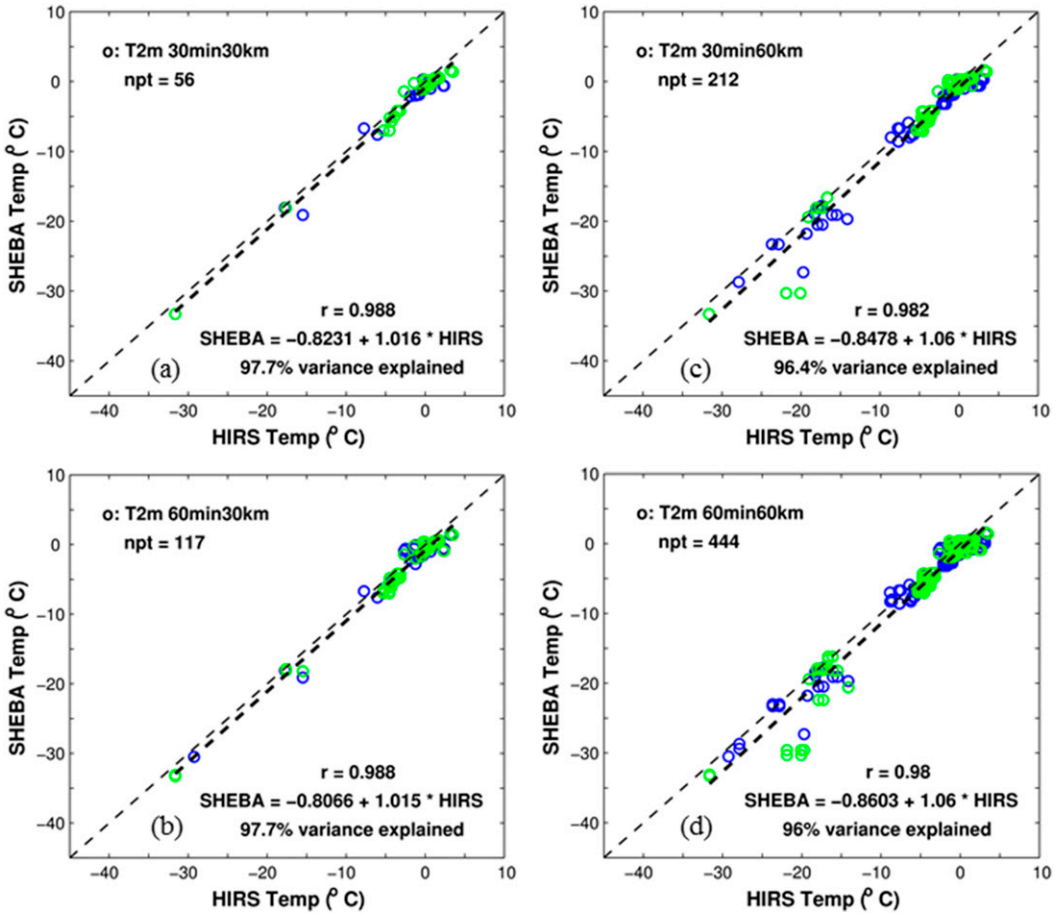

FIG. 3. As in Fig. 1, except that the overcast points based on SHEBA cloud fractions are excluded.

88% of SHEBA temperature variance explained by the linear regression of collocated HIRS temperatures.

The sensitivity to and importance of correctly identifying clear-sky pixels by a cloud mask to the HIRS temperature retrievals is clearly shown in this study. Because still more than 65% of cloud-screened HIRS records are potential overcast cells based on SHEBA cloud fractions and the fact that SHEBA data are limited in both space and time, this implies that having an accurate cloud mask within the comparable time and space scales of HIRS retrievals in the Arctic region is needed and essential to further improving HIRS temperature products.

The channels used in the HIRS retrievals are infrared channels. The persistent Arctic overcast conditions may limit the number of available true clear-sky data pixels in the region. However, the HIRS data should still augment measurements from the current station networks to provide additional spatial and temporal coverage. Furthermore, a remotely sensed surface air temperature product will have the benefit of providing regional characteristics and spatial variability away from the coastline and inhabited areas. This should help improve synoptic and seasonal forecasts by providing better representations of remote forcing in model initial conditions. The long-term consistent, accurate, and intercalibrated products are crucial in monitoring and understanding climate changes and facilitating the adaptation process. The analysis in this paper establishes a baseline of accuracy and uncertainty sources in HIRS near-surface air temperature retrievals and lays the groundwork for a remote sensing near-surface air temperature product in the Arctic.

Acknowledgments. This work is supported by NOAA's Climate Data Record program. G. Peng, S. Stegall, and J. Matthews are supported by NOAA under Cooperative Agreement NA14NES432003. We thank Ola Persson for information on the SHEBA composite data observations. Discussions with Ken Knapp, Robert Evans, Boyin Huang, and Huai-min Zhang are beneficial. Suggestions from Jay Lawrimore, Tom Maycock,

and the JTECH reviewers have improved the clarity of the manuscript.

REFERENCES

Bauer, P., L. Magnusson, J.-N. Thépaut, and T. M. Hamill, 2016: Aspects of ECMWF model performance in polar areas. *Quart. J. Roy. Meteor. Soc.*, doi:10.1002/qj.2449, in press.

Bourassa, M. A., and Coauthors, 2013: High-latitude ocean and sea ice surface fluxes: Challenges for climate research. *Bull. Amer. Meteor. Soc.*, **94**, 403–423, doi:10.1175/BAMS-D-11-00244.1.

Cavalieri, D. J., and C. L. Parkinson, 2012: Arctic sea ice variability and trends, 1979–2010. *Cryosphere*, **6**, 881–889, doi:10.5194/tc-6-881-2012.

Comiso, J. C., 2012: Large decadal decline of the Arctic multiyear ice cover. *J. Climate*, **25**, 1176–1193, doi:10.1175/JCLI-D-11-00113.1.

——, and F. Nishio, 2008: Trends in the sea ice cover using enhanced and compatible AMSR-E, SSM/I, and SMMR data. *J. Geophys. Res.*, **113**, C02S07, doi:10.1029/2007JC004257.

Cowtan, K., and R. G. Way, 2014: Coverage bias in the HadCRUT4 temperature series and its impact on recent temperature trends. *Quart. J. Roy. Meteor. Soc.*, **140**, 1935–1944, doi:10.1002/qj.2297.

Hassol, S. J., 2004: *Impacts of a Warming Arctic: Arctic Climate Impact Assessment*. Cambridge University Press, 140 pp.

Heidinger, A. K., M. J. Foster, A. Walther, and X. Zhao, 2014: The Pathfinder Atmospheres–Extended AVHRR climate dataset. *Bull. Amer. Meteor. Soc.*, **95**, 909–922, doi:10.1175/BAMS-D-12-00246.1.

Intrieri, J. M., M. D. Shupe, T. Uttal, and B. J. McCarty, 2002: An annual cycle of Arctic cloud characteristics observed by radar and lidar at SHEBA. *J. Geophys. Res.*, **107**, 8030, doi:10.1029/2000JC000423.

Jackson, D. L., and J. J. Bates, 2000: A 20-yr TOVS radiance Pathfinder data set for climate analysis. Preprints, *10th Conf. on Satellite Meteorology and Oceanography*, Long Beach, CA, Amer. Meteor. Soc., JP4.11. [Available online at https://ams.confex.com/ams/annual2000/techprogram/paper_5693.htm.]

Jeffries, M. O., J. Richter-Menge, and J. E. Overland, Eds., 2014: Arctic report card 2014. 75 pp. [Available online at http://www.arctic.noaa.gov/report14/ArcticReportCard_full_report.pdf.]

Karl, T. R., and Coauthors, 2015: Possible artifacts of data biases in the recent global surface warming hiatus. *Science*, **348**, 1469–1472, doi:10.1126/science.aaa5632.

NRC, 2001: *Enhancing NASA's Contributions to Polar Science: A Review of Polar Geophysical Data Sets*. National Academy Press, 138 pp., doi:10.17226/10083.

——, 2006: *Towards an Integrated Arctic Observing Network*. National Academies Press, 128 pp., doi:10.17226/11607.

Peng, G., W. N. Meier, D. J. Scott, and M. H. Savoie, 2013: A long-term and reproducible passive microwave sea ice concentration data record for climate studies and monitoring. *Earth Syst. Sci. Data*, **5**, 311–318, doi:10.5194/essd-5-311-2013.

Persson, P. O., C. W. Fairall, E. L. Andreas, P. S. Guest, and D. K. Perovich, 2002: Measurements near the Atmospheric Surface Flux Group tower at SHEBA: Near-surface conditions and surface energy budget. *J. Geophys. Res.*, **107**, 8045, doi:10.1029/2000JC000705.

Randall, D., and Coauthors, 1998: Status of and outlook for large-scale modeling of atmosphere–ice–ocean interactions in the Arctic. *Bull. Amer. Meteor. Soc.*, **79**, 197–219, doi:10.1175/1520-0477(1998)079<0197:SOAOFL>2.0.CO;2.

Rigor, I., R. L. Colony, and S. Martin, 2000: Variations in surface air temperature observations in the Arctic, 1979–97. *J. Climate*, **13**, 896–914, doi:10.1175/1520-0442(2000)013<0896:VISATO>2.0.CO;2.

Rothrock, D. A., and J. Zhang, 2005: Arctic Ocean sea ice volume: What explains its recent depletion. *J. Geophys. Res.*, **110**, C01002, doi:10.1029/2004JC002282.

Schweiger, A. J., R. W. Lindsay, J. A. Francis, J. Key, J. M. Intrieri, and M. D. Shupe, 2002: Validation of TOVS Path-P data during SHEBA. *J. Geophys. Res.*, **107**, 8041, doi:10.1029/2000JC000453.

Shi, L., 2011: Global atmospheric temperature and humidity profiles based on intersatellite calibrated HIRS measurement. *Ninth Conf. on Artificial Intelligence and Its Applications to the Environmental Sciences*, Seattle, WA, Amer. Meteor. Soc., J6.3. [Available online at https://ams.confex.com/ams/91Annual/webprogram/Paper179425.html.]

——, J. J. Bates, and C. Cao, 2008: Scene radiance–dependent intersatellite biases of HIRS longwave channels. *J. Atmos. Oceanic Technol.*, **25**, 2219–2229, doi:10.1175/2008JTECHA1058.1.

——, G. Peng, and J. Bates, 2012: Deriving surface temperature and humidity from long-term HIRS observation in high latitudes. *J. Atmos. Oceanic Technol.*, **29**, 3–13, doi:10.1175/JTECH-D-11-00024.1.

Stroeve, J. C., M. C. Serreze, M. M. Holland, J. E. Kay, J. Maslanik, and A. P. Barrett, 2012: The Arctic's rapidly shrinking sea ice cover: A research synthesis. *Climatic Change*, **110**, 1005–1027, doi:10.1007/s10584-011-0101-1.

U.S. CLIVAR Scientific Steering Committee, 2013: US Climate Variability and Predictability Program science plan. U.S. CLIVAR Project Office Rep. 2013-7, 85 pp.

Uttal, T., and Coauthors, 2002: Surface Heat Budget of the Arctic Ocean. *Bull. Amer. Meteor. Soc.*, **83**, 255–275, doi:10.1175/1520-0477(2002)083<0255:SHBOTA>2.3.CO;2.